

HIGH-DENSITY FLEXIBLE PARYLENE-BASED MULTIELECTRODE ARRAYS FOR RETINAL AND SPINAL CORD STIMULATION

D.C. Rodger^{1,2}, A.J. Fong¹, W. Li¹, H. Ameri², I. Lavrov³, H. Zhong³, S. Saati², P. Menon¹, E. Meng², J.W. Burdick¹, R.R. Roy³, V.R. Edgerton³, J.D. Weiland², M.S. Humayun², and Y.C. Tai¹

¹California Institute of Technology, Pasadena, CA, USA

(Tel: +1-626-395-8477; E-mail: dcrodger@mems.caltech.edu)

²University of Southern California, Los Angeles, CA, USA

³University of California, Los Angeles, Los Angeles, CA, USA

Abstract: Novel flexible parylene-based high-density electrode arrays have been developed for functional electrical stimulation in retinal and spinal cord applications. These electrode arrays are microfabricated according to single-metal-layer and, most recently, dual-metal-layer processes. A new heat-molding process has been implemented to conform electrode arrays to approximate the curvature of canine retinas, and chronic implantation studies have been undertaken to study the mechanical effects of parylene-based prostheses on the retina, with excellent results to date. Electrode arrays have also been implanted and tested on the spinal cords of murine models, with the ultimate goal of facilitation of locomotion after spinal cord injury; these arrays provide a higher density and better spatial control of stimulation and recording than is typically possible using traditional fine-wire electrodes. Spinal cord stimulation typically elicited three muscle responses, an early (direct), a middle (monosynaptic), and a late (polysynaptic) response, classified based on latency after stimulation. Stimulation at different rostrocaudal levels of the cord yielded markedly different muscle responses, highlighting the need for such high-density arrays.

Keywords: BioMEMS, Neural prosthesis, Parylene C, Retinal prosthesis.

1. INTRODUCTION

Prototype low-density retinal prostheses have shown great promise, enabling subjects blind from such diseases as retinitis pigmentosa and age-related macular degeneration to perceive visual data [1]. The next-generation retinal prosthesis (Fig. 1), however, requires a high-density flexible

electrode array and a high-lead-count cable to allow for high-resolution vision. We present the first flexible parylene-based multielectrode arrays (MEAs) designed for functional electrical stimulation (FES) in retinal prostheses, and the extension of this technology to enable stimulation of central nervous system structures after spinal cord injury. In addition, we present chronic biomechanical stability and acute neural stimulation results. We address the importance of a novel dual-metal-layer fabrication methodology that enables complex electrode arrangements while alleviating the traditional problems of electrode crowding due to wire-routing. The advantages of the use of parylene C as the structural material for such neuroprostheses, when compared with technologies based on the use of other materials such as polyimide [2] and silicon [3], include parylene's pinhole-free conformality, its low water permeability, its United States Pharmacopoeia (USP) Class VI biocompatibility, and its high flexibility and mechanical

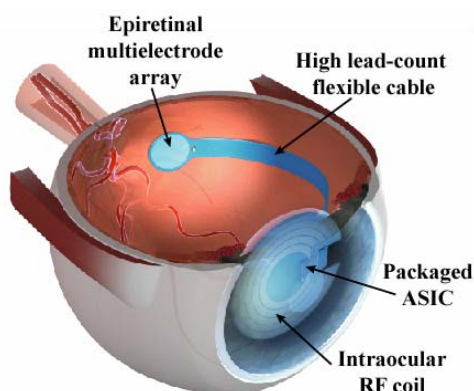


Fig. 1 Placement and components of next-generation retinal prosthesis.

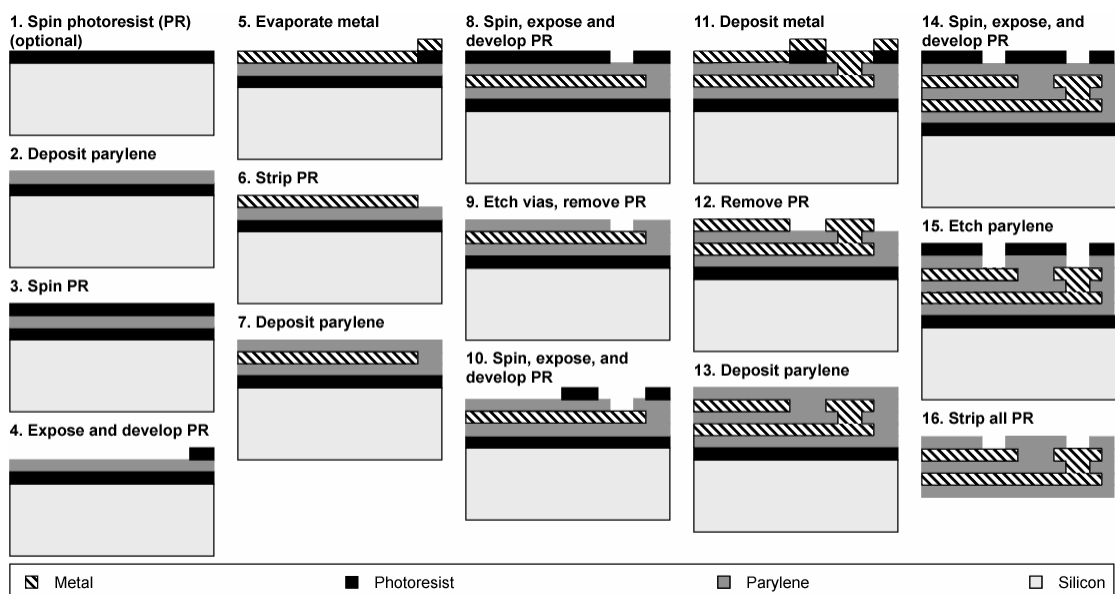


Fig. 2 Fabrication process for dual-metal-layer electrode arrays.

strength (Young's modulus ~ 4 GPa).

2. MICROFABRICATION

Single-metal-layer electrode arrays are fabricated as has been previously described [4]. Dual-layer electrode arrays are fabricated as shown in Fig. 2. Approximately $8\text{ }\mu\text{m}$ of parylene C is first deposited on a silicon wafer with an optional photoresist sacrificial layer, forming the underside of the electrode array. A platinum or titanium/platinum metal liftoff process is used to define traces with $16\text{ }\mu\text{m}$ pitch and 200 nm to 300 nm thickness. A second parylene deposition ($\sim 1\text{ }\mu\text{m}$) forms the insulation between the two metal layers. At this point, $6\text{ }\mu\text{m} \times 6\text{ }\mu\text{m}$ vias are patterned in the insulation layer over the ends of the traces using an oxygen plasma reactive-ion etch. A second step-coverage optimized liftoff process is used to define a second metal layer comprising electrodes and traces, while at the same time achieving electrical continuity between the underlying traces and the overlying electrodes. A final parylene coating approximately $7\text{ }\mu\text{m}$ thick forms the top insulation. The electrodes are exposed and the overall geometry of the implant is defined in a final set of reactive-ion etches using a thick photoresist etch mask. Finally, the arrays are peeled from the wafer in a water bath or released through removal of the sacrificial photoresist in acetone.

The implants are typically annealed for two

days at 200°C in a vacuum oven with nitrogen backfill to optimize parylene-parylene adhesion. In order to maintain the planarity of the spinal cord arrays, they are clamped between two flat pieces of Teflon or glass slides coated with aluminum foil. The retinal arrays, on the other hand, are shaped using a custom 6061 aluminum mold comprising a recessed concave region and a mating stainless steel sphere that approximates the curvature of the retina.

3. RESULTS

3.1 Fabricated devices

Retinal arrays consisting of 1024 $75\text{-}\mu\text{m}$ -diameter electrodes arranged in a complex biomimetic pattern that closely mimics the density of ganglion cells in the human retina [5] were fabricated according to the dual-layer process (Fig. 3a), with 60 of the electrodes connected via two traces each to facilitate electrical conductivity verification. The strength of metal adhesion was verified using a Scotch tape test. Electrical testing demonstrated a typical impedance of approximately $5\text{ k}\Omega$, which includes two $8\text{-}\mu\text{m}$ -wide traces of 20 mm length, as well as two via step junctions (vias are shown in Fig. 3b, a scanning electron micrograph of a single electrode). Each via has an impedance of less than $12.5\text{ }\Omega$. These arrays were successfully molded to the approximate curvature of the canine retina (Fig. 3c), and sterilized using ethylene oxide gas

prior to surgical implantation.

Spinal cord arrays, consisting of five or ten electrodes of 250 μm diameter (Fig. 4), were fabricated using the single-layer process. Interelectrode spacing was controlled so that each array covered four to five segments of the lumbosacral spinal cord.

3.2 Retinal chronic implantation

Our biomimetic arrays were implanted in the right eye of two canines through a 5-mm pars plana incision and were affixed to the retina using a retinal tack modified by the addition of a PDMS washer to account for the thin nature of the parylene-based arrays. They have remained chronically implanted for five and four months, respectively, and fluorescein angiography (FA) and optical coherence tomography (OCT) have demonstrated that the arrays are less than 50 μm away from the ganglion cell layer at the center and only slightly more raised at the edges, with normal retinal blood vessel filling underneath (Fig. 5).

3.3 Spinal cord electrical stimulation

Under isoflurane anesthesia, the spinal cord electrode arrays were implanted epidurally on spinal cord segments L2-S1 in nontransected

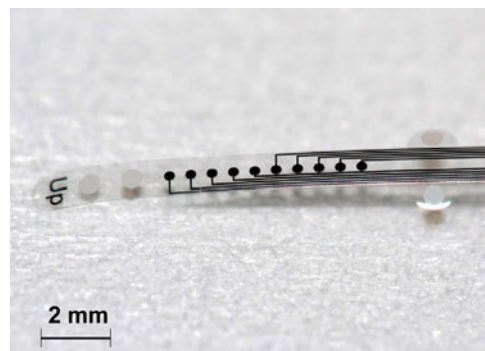


Fig. 4 Flexible electrode array for spinal cord stimulation and recording.

mice. The electrodes were oriented linearly along the rostrocaudal extent of the cord.

To test the capability of the electrode array to act as a multi-channel stimulating device for generating hindlimb movements, constant current monophasic stimulus pulses (amplitude: 50-850 μA , frequency: 0.3-10 Hz, pulse duration: 0.5 ms) were applied to the spinal cord via each of the array electrodes, while muscle activity was monitored using electromyogram (EMG) recordings of the tibialis anterior and medial gastrocnemius muscles. Stimulation generated a typical three-component EMG action potential consisting of an early (direct motor), a middle

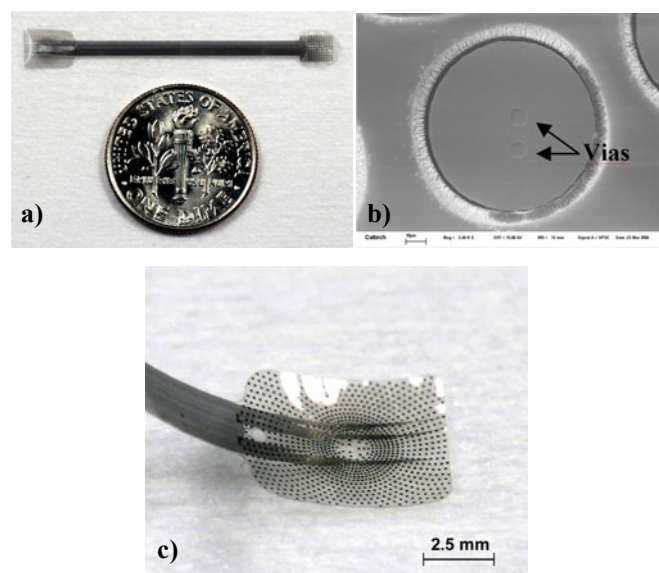


Fig. 3 a) Fabricated biomimetic electrode array with 60 of 1024 75- μm -diameter electrodes connected through dual-layer process; b) scanning electron micrograph of electrode highlighting vias to underlying traces; c) heat-molded and annealed retinal electrode array.

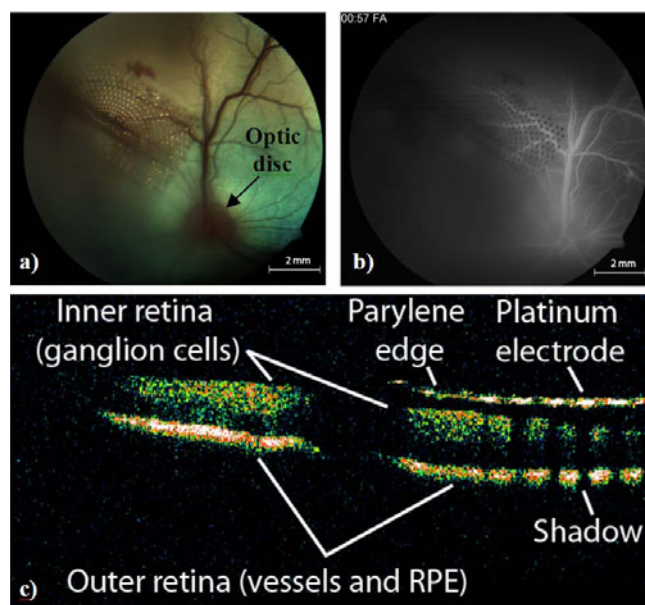


Fig. 5 a) Fundus photograph showing array tacked to the retina; b) FA showing normal blood flow under array and no leakage at the perimeter (no signs of retinal trauma); c) OCT showing bare retina at left and array in close apposition at right.

(monosynaptic), and a late (polysynaptic) response, classified by post-stimulus latency (Fig. 6). The appearance and magnitude of each of these responses was correlated with the choice of electrode position and stimulation parameters (Fig. 7).

Recording capability was assessed by using the electrode array to record spinal cord potentials evoked by tibial nerve stimulation. At different spinal cord levels, two or three distinct responses were observed. These findings closely mirror results reported previously in a study using conventional spinal cord recording electrodes [6].

4. CONCLUSION

These revolutionary parylene-based platinum multielectrode arrays have demonstrated the ability to stimulate and record from neural tissue, and have shown excellent biostability when chronically implanted in contact with canine retinas. The dual-metal-layer process enables increased electrode density while obviating many of the issues typically associated with single-layer arrays, such as those of electrode crowding due to increased electrode density and wire-routing. It is a simple matter to extend this process to increase the number of metal and parylene insulation layers. Future work includes the stimulation of retinal tissue using parylene-based arrays, development of two-dimensional arrays for bilateral spinal cord stimulation, and the fabrication of a completely integrated wireless stimulation system in a parylene substrate.

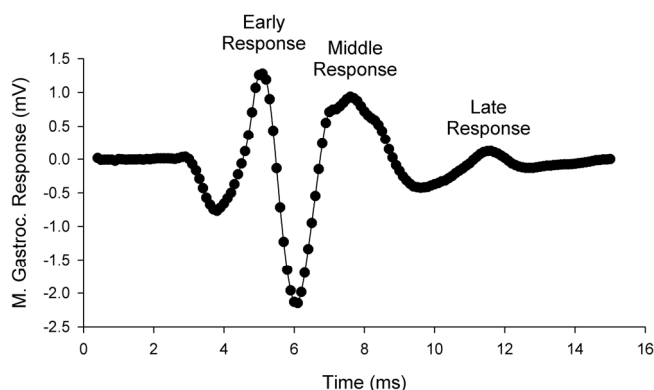


Fig. 6 Typical medial gastrocnemius (leg) EMG recording showing early, middle, and late responses after stimulation of spinal cord segments with parylene multielectrode array.

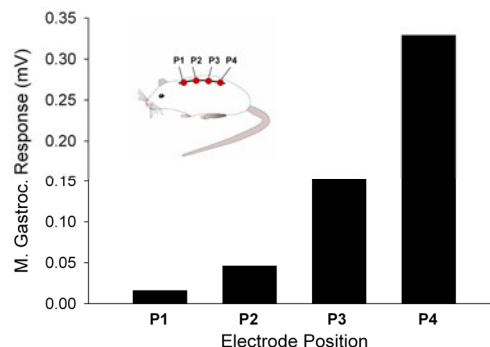


Fig. 7 Medial gastrocnemius EMG showing varying levels of activation caused by stimulation at different rostrocaudally located electrode sites.

5. ACKNOWLEDGMENTS

This work was supported in part by the Engineering Research Centers Program of the National Science Foundation under NSF Award Number EEC-0310723, and by a fellowship from the Whitaker Foundation (D.R.). The authors especially wish to thank Mr. Christian Gutierrez and Ms. Ronalee Lo for their help with the fabrication of the PDMS washers used with the retinal tacks, Mr. Andrew Pullin for his help with fabrication of the heat-forming mold, and Mr. Trevor Roper for his always valuable assistance.

REFERENCES

- [1] M. S. Humayun, J. D. Weiland, G. Y. Fujii, R. Greenberg, R. Williamson, J. Little, B. Mech, V. Cimarusti, G. Van Boemel, and G. Dagnelie, "Visual perception in a blind subject with a chronic microelectronic retinal prosthesis," *Vision Research*, vol. 43, pp. 2573-2581, 2003.
- [2] T. Stieglitz, W. Haberer, C. Lau, and M. Goertz, "Development of an inductively coupled epiretinal vision prosthesis," in *Digest Tech. Papers IEEE-EMBS Conference*, San Francisco, CA, USA, Sept. 1-5, 2004, pp. 4178-4181.
- [3] A. Hoogerwerf and K. Wise, "A three-dimensional microelectrode array for chronic neural recording," *IEEE Trans. Biomed. Eng.*, vol. 41, pp. 1136-1146, 1994.
- [4] D. C. Rodger, W. Li, H. Ameri, A. Ray, J. D. Weiland, M. S. Humayun, and Y. C. Tai, "Flexible parylene-based microelectrode technology for intraocular retinal prostheses," in *Digest Tech. Papers 1st IEEE-NEMS Conference*, Zhuhai, China, Jan. 18-21, 2006, pp. 745-748.
- [5] C. A. Curcio and K. A. Allen, "Topography of ganglion-cells in human retina," *Journal of Comparative Neurology*, vol. 300, pp. 5-25, 1990.
- [6] A. P. Chandran, K. Oda, H. Shibasaki, and M. Pisharodi, "Spinal somatosensory evoked potentials in mice and their developmental changes," *Brain & Development*, vol. 16, pp. 44-51, 1994.